Remote sensing constraints on South America fire traits by Bayesian fusion of atmospheric and surface data

A. Anthony Bloom[1], John Worden[1], Zhe Jiang[1], Helen Worden[2], Thomas Kurosu[1], Christian Frankenberg[1], David Schimel[1].

[1]Jet Propulsion Laboratory, California Institute of Technology, Pasadena, CA, U.S.A.

[2]Atmospheric Chemistry Division, National Center for Atmospheric Research, Boulder, CO, U.S.A.

Corresponding Author: A. Anthony Bloom, Jet Propulsion Laboratory, California Institute of Technology, Pasadena, CA, U.S.A. (abloom@jpl.nasa.gov)

@2014 All Rights Reserved

Accepted Article

This article has been accepted for publication and undergone full peer review but has not been through the copyediting, typesetting, pagination and proofreading process which may lead to differences between this version and the Version of Record. Please cite this article as doi: 10.1002/2014GL062584

©2015 American Geophysical Union. All rights reserved.

Abstract

Satellite observations reveal substantial burning during the 2007 and 2010 tropical South America fire season, with both years exhibiting similar total burned area. However, 2010 CO fire emissions, based on satellite CO concentration measurements, were substantially lower (-28%), despite the once-in-a-century drought in 2010. We use Bayesian inference with satellite measurements of CH_4 and CO concentrations and burned area to quantify shifts in combustion characteristics in 2010 relative to 2007. We find an 88% probability in reduced combusted biomass density associated with the 2010 fires, and an 82% probability of lower fire carbon losses in 2010 relative to 2007. Higher combustion efficiency was a smaller contributing factor to reduced 2010 CO emissions. The reduction in combusted biomass density is consistent with a reduction (4-6%) in GOME-2 solar induced fluorescence (a proxy for gross primary production) during the preceding months and a potential reduction in biomass (≤8.3%) due to repeat fires.

Key points:

- 2007 and 2010 were major fire years in tropical South America
- Lower-than-expected 2010 CO emissions despite a once-in-a-century drought
- 2010 fire carbon losses were likely low due to reduced biomass combustion rates

Index terms:

0365 Troposphere: composition and chemistry

0322 Constituent sources and sinks

0480 Remote sensing

0428 Carbon cycling

Keywords:

South America, biomass burning, TES, MOPITT, MODIS, carbon cycle

©2015 American Geophysical Union. All rights reserved.

Accepted Article

1. Introduction

Tropical fire carbon (C) losses, largely in the form of CO_2, CO and CH_4, amount to a significant portion of the global carbon budget. Tropical South America fires accounted for 5%-35% of annual tropical fire CO_2 emissions during 2001-2011 [Global Fires Emissions Database, van der *Werf et al.,* 2010]. Larger fire C losses typically occur during drier years [*Chen et al.,* 2013b]. For example, during the once-in-a-century 2010 Amazon drought [*Lewis et al.,* 2011], the combined effect of larger fires and reduced terrestrial C uptake resulted in a reversal of the net atmosphere-to-land C flux [*Gatti et al.,* 2014]. Fires can also have long-term effects on C cycling, resulting from increased tree mortality and shifts towards fire-resilient species [*Brando et al.,* 2014].

Emissions of CO_2, CO and CH_4 from fires are governed by the amount of available biomass C, the fraction of biomass C combusted (combustion completeness) and the fraction of combusted C emitted as CO_2 (combustion efficiency). Droughts can lead to changes in biomass burning traits, including reductions in fuel load [*Randerson et al.,* 2005; *Chen et al.,* 2013a] and fuel moisture [*Hély et al.,* 2003], which in turn will influence overall combustion efficiency and completeness [*Korontzi et al.,* 2003; *Hély et al.,* 2003; *Soares Neto et al.,* 2009]; these shifts can significantly alter large-scale fire C loss rates. Overall, placing top-down constraints on combustion characteristics and their inter-annual variations is essential to better quantify continental-scale terrestrial C exchange.

The relative scarcity of large-scale, repeat measurements of atmospheric CO_2 has posed a significant barrier to estimating C losses from tropical fires. CO and CH_4 are the next largest

©2015 American Geophysical Union. All rights reserved.

Accepted Article

gaseous forms of C loss from fires [*Andreae and Merlet*, 2001]. Based on in-situ measurements of the ratios of CO_2 to CO and CH_4 (or CO_2:CO:CH_4) within fire plumes, CO and CH_4 can provide a constraint on total C emissions. However CO and CH_4 emission factors vary amongst major land-cover types [*Andreae and Merlet*, 2001, *Akagi et al.*, 2011], and associated estimates of total C losses will inherently remain highly uncertain. Observations of burned area provide an independent constraint on fire C losses. Within burned areas, typically a high fraction of litter and foliar C is combusted, while coarser above-ground woody C is only partially combusted [*Ward et al.*, 1996; *Prasad et al.*, 2001]. The overall combustion completeness also varies as a result of fuel moisture [*Hély et al.*, 2003], fuel types [*Korontzi et al.*, 2003; *Soares Neto et al.*, 2009] amongst other attributes. As a result, biomass density and combustion completeness remain dominant sources of uncertainty in bottom-up C loss estimates. Ultimately, trace gas, biomass and burned area constraints can be used together to reduce uncertainties on fire C loss rates.

2. Remote-sensing constraints

Our study is focused on tropical South America (study region: 25°S – 5°S, 90°W – 30°W): according to the Global Fires Emissions Database [GFEDv3, *van der Werf et al.*, 2010] biomass burning within the study region amounts to 92% of total South America emissions during 2001-2011. Burned area within this region peaks during the dry season (July-October, Figure 1). We find large-scale agreements between the timing and magnitude of MODIS (Moderate Resolution Imaging Spectroradiometer) burned area [*Giglio et al.*, 2013], TES (Tropospheric Emission Spectrometer) CO retrievals (tes.jpl.nasa.gov) and MOPITT (Measurements Of Pollution In The Troposphere) CO V6J retrievals [*Worden et al.*, 2010; *Deeter et al.*, 2014]. Inter-annual variations in Tropical Rainfall Measuring Mission (TRMM)

©2015 American Geophysical Union. All rights reserved.

precipitation retrievals [*Huffman et al.*, 2007] and Gravity Recovery and Climate Experiment (GRACE) water storage retrievals [*Landerer and Swenson*, 2012] are broadly consistent with the dry-season CO and burned area magnitudes.

Two of the major fire years during this time period (2007 and 2010) exhibited similar burned areas (Figure 2a). However, in contrast to recent major droughts in 2005 and 2010 [*Lewis et al.*, 2011; *Gloor et al.*, 2013], 2007 was not a major drought year. The total above-ground biomass within the 2010 burned areas [*Saatchi et al.*, 2011] is 13% higher, and GFEDv3 bottom-up emission estimates amount to higher CO emissions (+24%) and higher total C loss (+23%) from 2010 fires, relative to 2007 [*van der Werf et al.*, 2010]. However, TES and MOPITT column integrated CO data (Figure 1) do not exhibit enhanced CO concentrations in 2010, relative to 2007. Moreover, CO inverse emission estimates based on MOPITT CO observations are 28% lower in 2010, relative to 2007 (Figure 2b). Details on the inverse CO emission estimates are provided in section 1 of the supplementary information (SI). Similarly, we find no significant enhancement in 2010 Ozone Monitoring Instrument (OMI) NO_2 concentrations relative to 2007 (Figure S3 in the SI).

We use the *Worden et al.* [2013a,b] approach to determine fire plume CH_4/CO ratios from Aura TES column-integrated CO and CH_4 observations over the study region. We find a higher 2010 CH_4/CO (0.11 g CH_4 g^{-1} CO) relative to 2007 (0.07-0.09 g CH_4 g^{-1} CO, see section 2 of the SI for details): this increase supports the explanation of a higher forest fire contribution to total CH_4 and CO emissions in 2010, because forest fires typically have a higher CH_4-to-CO ratio (i.e., higher CH_4/CO) relative to savanna and grassland fires [*Andreae and Merlet*, 2001] (see Figure 2c). However, the relative increase in forest fire emissions alone cannot account for a 28% decrease in CO emissions without a sizeable

©2015 American Geophysical Union. All rights reserved.

decrease in savanna and agricultural fire CO emissions. Likewise, elevated CH_4/CO in 2010 cannot be solely attributed to lower CO emission rates due to lower fuel moisture (i.e., higher combustion efficiency), as CH_4 and CO emissions factors are positively correlated [*Korontzi et al.*, 2003; *Soares Neto et al.*, 2009].

Therefore, lower-than-expected CO emissions in 2010 may have occurred as a result of a combined higher forest fire contribution and lower CO emission factors: a large-scale shift from smoldering to flaming fires [Soares Neto et al., 2009] may have resulted in increased combustion efficiency (i.e., lower CO emission rates). Alternatively, a 2010 decrease in combusted biomass density (biomass density × combustion completeness) may have resulted in both lower CO emissions and lower total fire C loss. A reduction in biomass may have occurred as a result of reduced gross primary production (GPP) during the 2010 wet season [*Lewis et al.*, 2011], which in turn could lead to a reduction in easily combustible fuel during the dry season [*Randerson et al.*, 2005; *Chen et al.*, 2013a].

To establish why in 2010, relative to 2007, burned area was higher (+5%) while 2010 CO emissions are lower (-28%), we use Bayesian inference to determine the probability of four hypotheses concerning a 2007-to-2010 increase/decrease in combustion efficiency and combusted biomass density: the hypotheses are summarized in Table 1. By quantifying the probability for each hypothesis, we can identify the likely underlying factors leading to greater burned area and less CO emissions in 2010, relative to 2007. Moreover, by quantifying the increase/decrease in combusted biomass density and combustion efficiency, we can quantify the difference between 2007 and 2010 fire C losses. We bring together (a) MOPITT CO concentrations; (b) TES CH_4/CO ratios; (c) MODIS burned area; (d) aboveground total biomass [*Saatchi et al.*, 2011]; and (e) land-cover type CO and CH_4

©2015 American Geophysical Union. All rights reserved.

emission factor prior information [*Andreae and Merlet*, 2001] together in a Bayesian inference framework to quantify changes in combusted biomass density (henceforth *CBD* = [combusted biomass]/[area]; units: kg C/m^2), modified combustion efficiency (henceforth *MCE* = [CO_2]/[CO_2 + CO + CH_4]; units: [kg C]/[kg C]) and total South America fire C losses in 2007 and 2010.

3. Estimates of burning coefficients

We express fire C fluxes of trace gas species *s* from land-cover type *b*, $F_{s,b}$, as:

$$F_{s,b} = A_b \times CBD_b \times E_{s,b} \quad (1)$$

where A_b, CBD_b and E_b are the burned area (m^2), combusted biomass density (kg C m^{-2}) within each land-cover type *b*, and $E_{s,b}$ is the corresponding carbon emission factor (kg C species per kg C combusted) for each trace gas species *s* within each land-cover type *b*. BCD_b can be expressed as

$$CBD_b = C_b \times B_b \quad (2)$$

where C_b and B_b are the combustion completeness and biomass density in land-cover type b, respectively. We express modified combustion efficiency (MCE_b) as

$$MCE_b = 1 - E_{CO,b} - E_{CH4,b} \quad (3)$$

©2015 American Geophysical Union. All rights reserved.

given that biomass burning C losses other than CH_4, CO_2 and CO emissions are negligible [*Andreae and Merlet*, 2001].

We determine the total burned area in 2007 and 2010 (A_b) during the fire season (May-Dec) for each land-cover type from the *Giglio et al.*, [2013] MODIS burned area 0.25° × 0.25° gridded product: based on the burned area land-cover types, we determine the A_b for three major land-cover type groups: savannas & grasslands, forests, and agriculture. We treat CBD_b^y and $E_{s,b}^y$ (for s = [CO, CH_4]; for b = [1. savanna & grasslands, 2. forest, 3. agriculture]; for y = [2007,2010]) as unknown quantities (henceforth parameter vector **x**). Based on the study-region scale observations **O,** which consist of CO and CH_4 observational constraints (total May-December 2007, 2010 MOPITT derived CO emissions and monthly TES CH_4/CO ratios) we use Bayesian inference to derive the probability density function of **x** given **O**, p(**x**|**O**), as follows:

$$p(\mathbf{x}|\mathbf{O}) \propto p(\mathbf{O}|\mathbf{x})\, p(\mathbf{x}) \qquad (4)$$

where p(**O**|**x**) is the probability of **O** given **x**, and p(**x**) is the prior probability of **x**. For a given parameter vector **x**, p(**O**|**x**) is determined by comparing study-area integrated fluxes ($\sum_{b=1}^{3} F_{CO,b}$ and $\sum_{b=1}^{3} F_{CH4,b}$) against TES CH_4/CO and total MOPITT-derived CO emission estimates and their associated uncertainty characteristics. For a given parameter vector **x**, p(**x**) consists of prior constraints on CBD_b^y and $E_{s,b}^y$ and their associated uncertainty characteristics. We use a Metropolis Hastings Markov Chain Monte Carlo approach (MHMCMC) [e.g., *Ziehn et al.*, 2012; *Bloom and Williams* 2014] to derive 2×10^5 samples of **x**; based on their distribution, we derive the probability density functions of CBD_b^y and

©2015 American Geophysical Union. All rights reserved.

$E_{s,b}^{y}$. Details on the observational and prior constraints, their associated uncertainties and the MHMCMC approach are included in section 3 of the supplementary information.

From 2 × 10^5 samples of CBD_b^y and $E_{s,b}^{y}$, we determine the region-wide overall combusted biomass density (CBD^y) and modified combustion efficiency (MCE^y) for years y (y = 2007, 2010), as follows:

$$CBD^y = \frac{\sum_{b=1}^{3} A_b^y \, BCD_b^y}{\sum_{b=1}^{3} A_b^y}, \; MCE^y = \frac{\sum_{b=1}^{3}\left(1-E_{CH_4,b}^{y}-E_{CO,b}^{y}\right)A_b^y BCD_b^y}{\sum_{b=1}^{3} A_b^y BCD_b^y} \qquad (5)$$

We also determine the probability density function of the carbon fluxes for each vegetation type based on the 2 × 10^5 CBD_b samples. We calculate total C losses F_C as the overall sum of total C losses ($A_b \times CBD_b$) from savanna, forest and agriculture fires. We determine individual land-cover type and region-wide probabilities for hypotheses 1-4 as follows:

Probability of H_N = [No. of samples **x** where H_N is true]/[2 × 10^5] × 100%. (6)

4. Combusted biomass density, efficiency and C losses

Table 2 describes the probability of 2007-to-2010 changes in combusted biomass density [*CBD*: gC combusted/burned area] and modified combustion efficiency [*MCE*: kg C (CO_2)/kg C (CO + CH_4 + CO_2)]. For example there is a 25% probability that both *CBD* and *MCE* increased in 2010 within savanna fires, as shown in the 'H1' row and 'savanna' column of Table 2. Within the whole study area, we find that lower *CBD* and higher *MCE* – Hypothesis 2 – is the most probable cause for lower CO emissions and larger burned area in

©2015 American Geophysical Union. All rights reserved.

2010, relative to 2007 (H2: 60%, see Figure 3). In particular, a change in forest and savanna fire characteristics likely explains the reduced CO emissions: with 47% and 55% probabilities that there was a both reduction in *CBD* and an increase in *MCE* within these fires. While it is possible that there is an increase in *CBD* and a decrease in *MCE* within each of the three regions separately, there is a 0% probability that all three regions have this same change in fire characteristics. The probability density function of 2007-to-2010 changes in *MCE* and *CBD* are shown in Figure 3. We could not resolve the probable changes in agricultural combustion traits (H1: 26%, H2: 28%, H3: 24%, H4: 22%), likely because these is a relatively small contribution to total C emissions from agricultural fires in both years (A_{agr} was 20% and 22% of total burned area in 2007 and 2010).

The hypothesis 1-4 probabilities depend on the uncertainties for the combusted biomass density and emission factor parameters in Equation 1 (CBD_b and $E_{s,b}$), as well as the observation uncertainties; these are reported in sections 3 of the supplementary information. The uncertainties that most strongly affect these outcomes are those related to the mean and the 2007-to-2010 change in the Equation 1 parameters. For example, we currently assume a one-sigma probability that fire characteristics will change by less than a factor of two between 2007 and 2010. This is a conservative estimate of inter-annual variations in fire characteristics, based on the seasonal range of reported combustion factor and efficiency measurements [e.g., *Korontzi et al.*, 2003; *Hély et al.*, 2003], as we are not aware of any inter-annual measurements of these parameters. However, even when we increase this uncertainty by a factor of two, our overall conclusions remain unchanged (Table 3 in Section 4 of SI). Additional potential sources of error in our simple model (equation 1) include biases in MODIS derived total fire-season burned area and land-cover classifications [*Giglio et al.*, 2013]. We also note the potential effect of seasonal changes in *CBD* and *MCE*: biomass

©2015 American Geophysical Union. All rights reserved.

burning combustion factor and efficiency can vary significantly on monthly timescales [*Korontzi et al.*, 2005].

Discussion and implications

If we combine the outcomes for the change in combusted biomass density (gC combusted/burned area) and modified combustion efficiency (CO_2 /[CO + CH_4 + CO_2]) with the change in burned area (equation 1), we find that total C emissions were likely lower by ~119 Tg C in 2010 relative to 2007 (Figure 3). However, there is a non-zero (17.6%) probability of an increase in carbon emissions. In contrast, the bottom-up (or GFEDv3) fire emissions were higher by +123 Tg C in 2010, relative to 2007.

For the whole study area, the probability of a 2007-to-2010 combusted biomass density reduction (H1 & H2) is 88%, and the probability of a modified combustion efficiency increase (H2 & H3) is 72% (Figure 3). The 2007-to-2010 increase in modified combustion efficiency (median increase = +0.01) is consistent with observed increases in combustion efficiency due to drier fuel conditions [*Korontzi et al.*, 2003; *Soares Neto et al.*, 2009]. The median 2007-to-2010 combusted biomass density reduction is 22%: based on equation 2, this reduction corresponds to either (a) a 22% reduction in biomass density, or (b) a 22% reduction in the combustion completeness, or (c) a combined change in both. We next discuss the potential 2007-to-2010 changes in biomass and/or combustion completeness.

Reduced productivity during the regional drought in 2010 may have led to a reduction in biomass available for combustion: as a large proportion of biomass loss from fires is derived from leaf and wood litter C, a reduction in the preceding wet-season GPP and corresponding

©2015 American Geophysical Union. All rights reserved.

fuel load [e.g., *Randerson et al.,* 2005] is a viable cause for a reduction of CO and fire C losses in 2010 shown in Figure 3. We find a 4-6% reduction in GOME-2 measurements of solar induced fluorescence (henceforth *SIF*) [*Joiner et al.,* 2013] in 2010 relative to 2007 during the time period preceding the major fires (February-June) within the study area (see section 7 of the SI). *SIF* is a proxy for *GPP* [*Frankenberg et al.,* 2011], which in turn determines the fuel load during the subsequent fire season [e.g., *Randerson et al.,* 2005]. Reduction in biomass density between 2007 and 2010 may have also occurred due to repeat fires and deforestation; we estimate that repeat fires could amount for up to an 8.3% reduction in biomass within burned areas between 2007 and 2010 (see section 5 of the SI).

Combustion completeness (the fraction of biomass burned) is typically expected to increase as a result of drier conditions [*Hély et al.,* 2003; *Korontzi et al.,* 2005; *van der Werf et al.,* 2010]. However, a reduction in GPP, leading to less combustible fuel, could in turn lead to diminished fire persistence, [e.g., *Giglio et al.,* 2006] therefore effectively suppressing large-scale combustion completeness within burned areas. Overall reductions in biomass and combustion completeness are both possible explanations for a reduction in combusted biomass density, and we currently do not have the large-scale constraints needed to differentiate between the two. We therefore require further data constraints to better quantify trends in fire C losses, and biomass burning characteristics.

Orbiting Carbon Observatory-2 (OCO-2) XCO_2 data [*Crisp et al.,* 2008] will place stronger constraints on the inter-annual carbon emissions from fires. For example, both a 2007-to-2010 increase or decrease of combusted biomass density are possible, as shown in Table 2. Currently combusted biomass density is indirectly constrained by the CO and CH_4 from MOPITT and TES, but these trace gases represent 2%-9% of carbon in biomass burning

©2015 American Geophysical Union. All rights reserved.

emissions. XCO_2 derived CO_2 fluxes would place a stronger constraint on combusted biomass density. Similarly, XCO_2 data from biomass burning plumes would place stronger constraints on combustion efficiency. Satellite derived above-ground biomass data, such as the future Global Ecosystem Dynamics Investigation Lidar (GEDI) and BIOMASS missions [*Krainak et al.*, 2012; *Hélière et al.*, 2014], can also be used to de-convolve changes in biomass density and combustion completeness.

Acknowledgments

Part of this research was carried out at the Jet Propulsion Laboratory, California Institute of Technology, under a contract with the National Aeronautics and Space Administration. TES CH_4 and CO data products are available at tes.jpl.nasa.gov. The MODIS burned area product was obtained from modis-fire.umd.edu. The NCAR MOPITT project is supported by the National Aeronautics and Space Administration (NASA) Earth Observing System (EOS) Program. We are grateful for feedback from F. Landerer and J. Joiner on our use of GRACE and GOME-2 data.

References

Akagi, S. K., et al. (2011). Emission factors for open and domestic biomass burning for use in atmospheric models. *Atmospheric Chemistry and Physics*, *11*(9), 4039-4072. doi:10.5194/acp-11-4039-2011

Andreae, M. O., and Merlet, P. (2001). Emission of trace gases and aerosols from biomass burning. *Global Biogeochemical Cycles*, *15*(4), 955-966. doi: 10.1029/2000GB001382

©2015 American Geophysical Union. All rights reserved.

Bloom, A. A., and Williams, M. (2014). Constraining ecosystem carbon dynamics in a data-limited world: integrating ecological "common sense" in a model-data-fusion framework. *Biogeosciences Discussions*, *11*(8), 12733-12772. doi:10.5194/bgd-11-12733-2014

Brando, P. M., et al. (2014). Abrupt increases in Amazonian tree mortality due to drought–fire interactions. *Proceedings of the National Academy of Sciences*, *111*(17), 6347-6352. doi: 10.1073/pnas.1305499111

Chen, Y., et al. (2013a). Long-term trends and interannual variability of forest, savanna and agricultural fires in South America. *Carbon Management*, *4*(6), 617-638. doi:10.4155/cmt.13.61

Chen, Y., Velicogna, I., Famiglietti, J. S., and Randerson, J. T. (2013b). Satellite observations of terrestrial water storage provide early warning information about drought and fire season severity in the Amazon. *Journal of Geophysical Research: Biogeosciences*, *118*(2), 495-504. doi: 10.1002/jgrg.20046

Crisp, D., DeCola, P. L., and Miller, C. E. (2008). NASA Orbiting Carbon Observatory: measuring the column averaged carbon dioxide mole fraction from space. *Journal of Applied Remote Sensing*, *2*(1), 023508-023508. doi:10.1117/1.2898457

Deeter, M. N., et al., (2014). The MOPITT Version 6 product: algorithm enhancements and validation. *Atmospheric Measurement Techniques Discussions*, *7*(6), 6113-6139. doi:10.5194/amtd-7-6113-2014

Frankenberg, C., et al., (2011). New global observations of the terrestrial carbon cycle from GOSAT: Patterns of plant fluorescence with gross primary productivity. *Geophysical Research Letters*, *38*(17). doi: 10.1029/2011GL048738

Gatti, L. V., et al. (2014). Drought sensitivity of Amazonian carbon balance revealed by atmospheric measurements. *Nature*, *506*(7486), 76-80. doi:10.1038/nature12957

Accepted Article

©2015 American Geophysical Union. All rights reserved.

Giglio, L., Van der Werf, G. R., Randerson, J. T., Collatz, G. J., and Kasibhatla, P. (2006). Global estimation of burned area using MODIS active fire observations. *Atmospheric Chemistry and Physics*, *6*(4), 957-974. doi: 10.5194/acp-6-957-2006

Giglio, L., Randerson, J. T., and van der Werf., G. R., (2013). Analysis of daily, monthly, and annual burned area using the fourth‐generation global fire emissions database (GFED4). *Journal of Geophysical Research: Biogeosciences* 118: 317-328, doi:10.1002/jgrg.20042.

Gloor, M., Brienen, R. J. W., Galbraith, D., Feldpausch, T. R., Schöngart, J., Guyot, J‐L., Espinoza, J. C., Lloyd, J., and Phillips, O. L. (2013) "Intensification of the Amazon hydrological cycle over the last two decades." *Geophysical Research Letters* 40(9), 1729-1733, doi: 10.1002/grl.50377

Hély, C., Alleaume, S., Swap, R. J., and Justice, C. O. (2003). SAFARI-2000 characterization of fuels, fire behavior, combustion completeness, and emissions from experimental burns in infertile grass savannas in western Zambia. *Journal of Arid Environments*, *54*(2), 381-394. doi: 10.1006/jare.2002.1097

Hélière, F., Fois, F., Arcioni, M., Bensi, P., Fehringer, M., and Scipal, K. (2014, June). Biomass P-band SAR interferometric mission selected as 7th Earth Explorer Mission. *EUSAR 2014; Proceedings of 10th European Conference on Synthetic Aperture Radar;* (pp. 1-4). VDE.

Huffman, G. J., et al. (2007). The TRMM multisatellite precipitation analysis (TMPA): Quasi-global, multiyear, combined-sensor precipitation estimates at fine scales. *Journal of Hydrometeorology*, *8*(1), 38-55. doi: 10.1175/JHM560.1

Joiner, J., et al. (2013). Global monitoring of terrestrial chlorophyll fluorescence from moderate-spectral-resolution near-infrared satellite measurements: methodology, simulations, and application to GOME-2. *Atmospheric Measurement Techniques*, *6*(10), 2803-2823. doi:10.5194/amt-6-2803-2013

Accepted Article

©2015 American Geophysical Union. All rights reserved.

Korontzi, S., et al. (2003). Seasonal variation and ecosystem dependence of emission factors for selected trace gases and PM2. 5 for southern African savanna fires. *Journal of Geophysical Research: Atmospheres (1984–2012)*, *108*(D24). doi: 10.1029/2003JD003730

Krainak, M. A., et al. (2012). Laser transceivers for future NASA missions. *Proc. SPIE* (pp. 83810Y-83810Y). doi:10.1117/12.920783

Landerer, F. W., and Swenson, S. C. (2012). Accuracy of scaled GRACE terrestrial water storage estimates. *Water Resources Research*, *48*(4). doi: 10.1029/2011WR011453

Lewis, S. L., Brando, P. M., Phillips, O. L., van der Heijden, G. M., and Nepstad, D. (2011). The 2010 amazon drought. *Science*, *331*(6017), 554-554. doi: 10.1126/science.1200807

Prasad, V. K., Kant, Y., Gupta, P. K., Sharma, C., Mitra, A. A., and Badarinath, K. V. S. (2001). Biomass and combustion characteristics of secondary mixed deciduous forests in Eastern Ghats of India. *Atmospheric Environment*, *35*(18), 3085-3095. doi:10.1016/S1352-2310(01)00125-X

Randerson, J. T., Van der Werf, G. R., Collatz, G. J., Giglio, L., Still, C. J., Kasibhatla, P., J. B. Miller, J. W. C. White, R. S. DeFries, and Kasischke, E. S. (2005). Fire emissions from C3 and C4 vegetation and their influence on interannual variability of atmospheric CO2 and δ13CO2. *Global Biogeochemical Cycles*, *19*(2). doi: 10.1029/2004GB002366

Saatchi, S. S., et al. (2011). Benchmark map of forest carbon stocks in tropical regions across three continents. *Proceedings of the National Academy of Sciences*, *108*(24), 9899-9904. doi:10.1073/pnas.1019576108

Soares Neto, T. G., et al. (2009). Biomass consumption and CO2, CO and main hydrocarbon gas emissions in an Amazonian forest clearing fire. *Atmospheric Environment*, *43*(2), 438-446. doi:10.1016/j.atmosenv.2008.07.063

Accepted Article

©2015 American Geophysical Union. All rights reserved.

van der Werf, G. R., et al. (2010). Global fire emissions and the contribution of deforestation, savanna, forest, agricultural, and peat fires (1997–2009). *Atmospheric Chemistry and Physics*, *10*(23), 11707-11735. doi:10.5194/acp-10-11707-2010

Ward, D. E., Hao, W. M., Susott, R. A., Babbitt, R. E., Shea, R. W., Kauffman, J. B., and Justice, C. O. (1996). Effect of fuel composition on combustion efficiency and emission factors for African savanna ecosystems. *Journal of Geophysical Research: Atmospheres (1984–2012)*, *101*(D19), 23569-23576. doi: 10.1029/95JD02595

Worden, H. M., Deeter, M. N., Edwards, D. P., Gille, J. C., Drummond, J. R., and Nédélec, P. (2010). Observations of near-surface carbon monoxide from space using MOPITT multispectral retrievals. *Journal of Geophysical Research: Atmospheres (1984–2012)*, *115*(D18). doi: 10.1029/2010JD014242

Worden, J., et al. (2013a). CH4 and CO distributions over tropical fires during October 2006 as observed by the Aura TES satellite instrument and modeled by GEOS-Chem. *Atmospheric Chemistry and Physics*, *13*(7), 3679-3692. doi:10.5194/acp-13-3679-2013

Worden, J., et al. (2013b). El Niño, the 2006 Indonesian peat fires, and the distribution of atmospheric methane. *Geophysical Research Letters*, *40*(18), 4938-4943. doi: 10.1002/grl.50937

Ziehn, T., Scholze, M., and Knorr, W. (2012). On the capability of Monte Carlo and adjoint inversion techniques to derive posterior parameter uncertainties in terrestrial ecosystem models. *Global Biogeochemical Cycles*, *26*(3). doi: 10.1029/2011GB004185

Accepted Article

©2015 American Geophysical Union. All rights reserved.

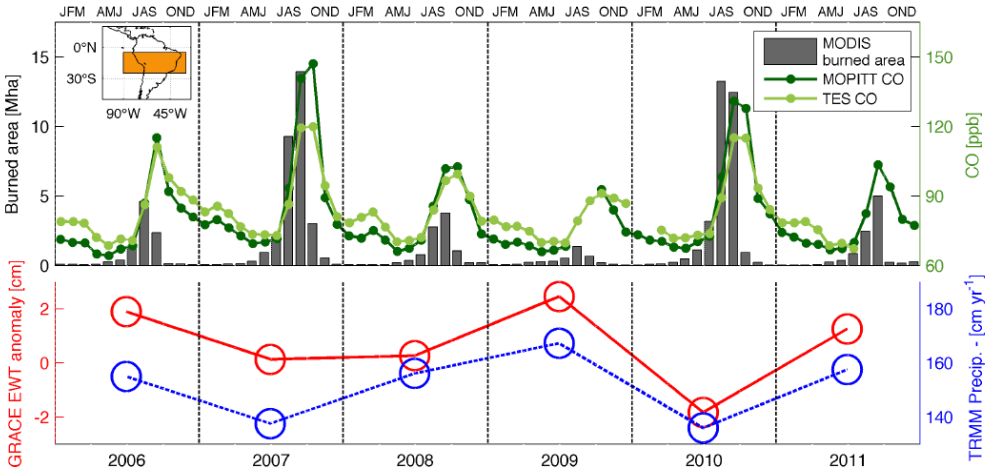

Figure 1. Top panel: monthly MODIS burned area (dark grey), MOPITT CO (dark green) and TES CO (light green) during 2006-2011 within the study area. Inset: map showing the tropical South America study area. Bottom panel: annual mean GRACE equivalent water height (EWT) and TRMM total precipitation within the study area.

Accepted Article

©2015 American Geophysical Union. All rights reserved.

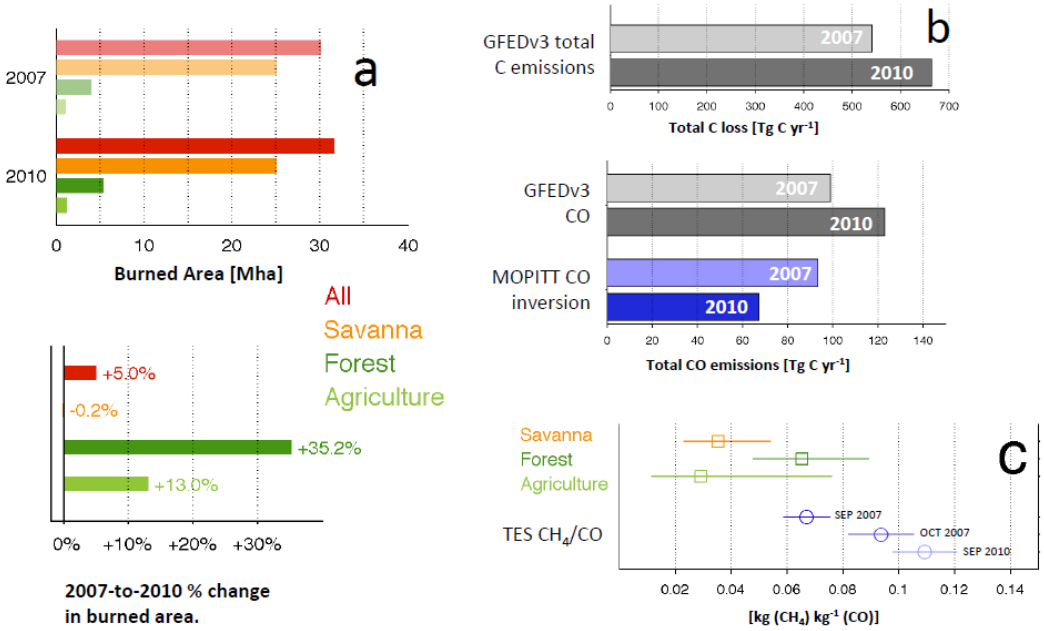

Figure 2. Panel **a**: Savanna, forest, agriculture and total burned area (top) and 2007-to-2010 % changes in total burned area within the study region (bottom). Panel **b**: bottom-up (GFEDv3) 2007 and 2010 total fire C emissions (top); bottom-up (GFEDv3) and top-down (MOPITT) estimates of 2007 and 2010 fire CO within the study area. Panel **c**: Land-cover specific CH_4/CO mass ratios and associated uncertainties, for savanna, forest and agriculture fires emissions; TES CH_4/CO ratios based on monthly TES column-integrated CO and CH_4 concentrations within the study area.

Accepted

©2015 American Geophysical Union. All rights reserved.

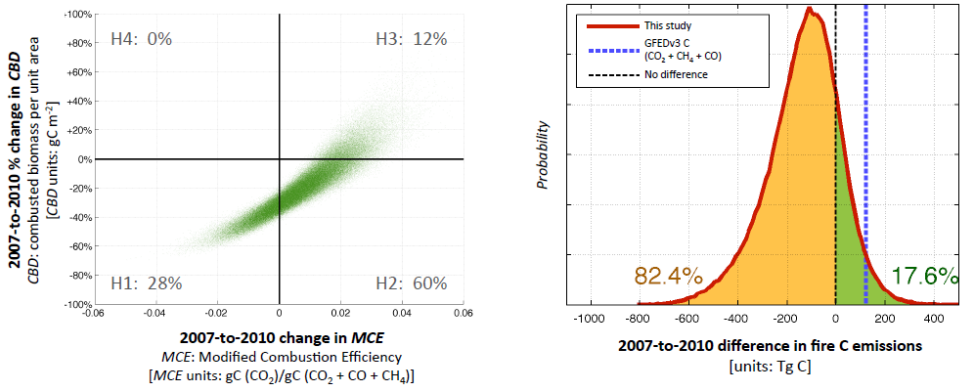

Figure 3. Left panel: probability distribution of 2007-to-2010 combusted biomass density change (CBD, y-axis) and combustion efficiency change (MCE, x-axis) within the study area. Positive changes in *MCE* correspond to a decrease in CO emission factors between 2007 and 2010. The probabilities of hypotheses 1-4 (Table 1) are shown within each quadrant. Right panel: 2007-to-2010 difference in biomass burning total C emissions based on optimized *CBD* values, in comparison to bottom-up 2010-2007 total C emissions difference (based on total GFEDv3 CO_2 + CO + CH_4 from savanna, forest and agriculture fires); the orange/green numbers denote the top-down probability of less/more total C emissions from 2010 fires relative to 2007 fires.

Accepted Article

©2015 American Geophysical Union. All rights reserved.

Table 1: Hypotheses 1-4[a]

Hypotheses	Change in 2010 combusted biomass density (*CBD*) and combustion efficiency (*MCE*), relative to 2007
H1	Decrease in *CBD* and decrease in *MCE*.
H2	Decrease in *CBD* and increase in *MCE*.
H3	Increase in *CBD* and increase in *MCE*.
H4	Increase in *CBD* and decrease in *MCE*.

[a]Hypotheses 1-4 outline all combinations of combusted biomass density (*CBD*, [combusted biomass]/[area]; units: kg/m^2) and modified combustion efficiency (*MCE*, [CO_2]/[CO_2 + CO + CH_4]; units: kg C/kg C) changes between 2007 and 2010.

Accepted Article

©2015 American Geophysical Union. All rights reserved.

Table 2: probability of hypotheses 1-4[b]

Hypothesis	2010-2007 *CBD* and *MCE* change	**Savanna**	**Forests**	**Agriculture**	**Whole study area.**
		Hypothesis probability			
H1	*CBD* ↓ *MCE* ↓	25%	19%	26%	**28%**
H2	*CBD* ↓ *MCE* ↑	47%	55%	28%	**60%**
H3	*CBD* ↑ *MCE* ↑	19%	17%	24%	**12%**
H4	*CBD* ↑ *MCE* ↓	8%	9%	22%	**0%**

[b]Probabilities of hypotheses 1-4 (see Table 1) based on Bayesian inference of combusted biomass density (*CBD*) and modified combustion efficiency (*MCE*): land-surface and atmospheric constraints on fire C emissions were used to calculate optimal 2007 and 2010 *CBD* and *MCE* values.

Accepted Article

©2015 American Geophysical Union. All rights reserved.